

StableKD: Breaking Inter-block Optimization Entanglement for Stable Knowledge Distillation

Shiu-hong Kao*, Jierun Chen*, S.H. Gary Chan

The Hong Kong University of Science and Technology

{skao, jcheneh, gchan}@cse.ust.hk

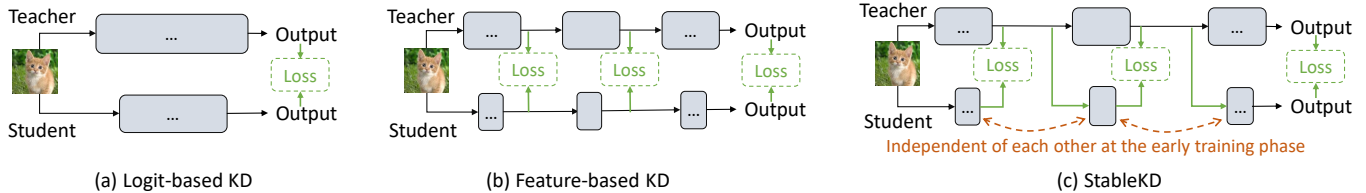


Figure 1: Comparison of StableKD with vanilla logit-based and feature-based knowledge distillation frameworks.

Abstract

Knowledge distillation (KD) has been recognized as an effective tool to compress and accelerate models. However, current KD approaches generally suffer from an accuracy drop and/or an excruciatingly long distillation process. In this paper, we tackle the issue by first providing a new insight into a phenomenon that we call the *inter-block optimization entanglement* (IBOE), which makes the conventional end-to-end KD approaches unstable with noisy gradients. We then propose StableKD, a novel KD framework that breaks the IBOE and achieves more stable optimization. StableKD distinguishes itself through two operations: *Decomposition* and *Recomposition*, where the former divides a pair of teacher and student networks into several blocks for separate distillation, and the latter progressively merges them back, evolving towards end-to-end distillation. We conduct extensive experiments on CIFAR100, Imagewoof, and ImageNet datasets with various teacher-student pairs. Compared to other KD approaches, our simple yet effective StableKD greatly boosts the model accuracy by 1% – 18%, speeds up the convergence up to 10 \times , and outperforms them with only 40% of the training data.

1 Introduction

While the great potential of deep learning has been showcased by many large-scale models running on the cloud [Devlin *et al.*, 2018; Holcomb *et al.*, 2018], a burgeoning direction is to bring the intelligence to the edge, by building

compact and computation-efficient models. Knowledge Distillation (KD), among various branches of methods, is well-known for its conceptual simplicity and ease of implementation. KD aims to distill knowledge from a large-scale teacher model to a smaller and faster student model. A typical vanilla KD approach provides the informative “soft targets” from the last layer of the teacher to the student [Hinton *et al.*, 2015]. The feature-based KD approaches further enforce the alignment of intermediate feature maps [Heo *et al.*, 2019a; Jung *et al.*, 2021]. Though effective in downsizing the model and reducing the computational complexity, they generally lead to deterioration in accuracy, leaving an accuracy gap between the teacher and the student. Beyer *et al.* [2022] narrow down the gap by distilling patiently for a large number of epochs. However, such an excruciatingly long distillation process is costly in terms of computational resources and energy. The situation can worsen when the task becomes more complex, involving a huge training dataset. Collectively, these factors diminish the appeal of KD for intensive and practical deployment.

How can we improve a student’s accuracy and simultaneously accelerate the KD process? We probe into the problem from a closely related optimization perspective. Given a student network composed of a series of blocks¹, current KD approaches mainly train it in an end-to-end manner. Therefore, the optimization of a block is conditioned on or entangled with other blocks by noisy gradients. We call this phenomenon *inter-block optimization entanglement* (IBOE). We hypothesize that such entanglement can incur optimization instability especially when the randomly initialized parameters are far from convergence at the early training phase. The optimization instability will then lead to accuracy fluctuation and slow down the convergence [Shalev-Shwartz *et al.*, 2017].

*These authors contributed equally.

¹A block refers to a layer or a stack of consecutive layers in a

The above observation motivates us to propose a novel KD framework that has a more stable optimization – StableKD. It consists of two operations, *Decomposition* and *Recomposition*. *Decomposition* breaks the IBOE by dividing a pair of teacher and student networks into separate blocks. Notably the input of a student block is identical to the input of its corresponding teacher block, rather than the output of its preceding student block. This simple design essentially differentiates StableKD from prior works, as shown in Figure 1. It enables the student blocks to learn independently, stably, and rapidly from their teacher. However, it incurs an architectural discrepancy between training and inference, i.e., the student blocks are blind to each other during training but have to collaborate for inference. Such discrepancy, as verified in the paper, can adversely affect the student’s final accuracy. To overcome this side effect, *Recomposition* is imposed to progressively merge the divided blocks back along the training process. This is reasonable as the student blocks get more mature after certain epochs, and the IBOE becomes less of a concern.

As such, we keep our StableKD framework simple yet effective in increasing the optimization stability, and thereby boosting the model accuracy and accelerating the KD process. We conduct experiments on the widely adopted CIFAR100 [Krizhevsky, 2009], Imagewoof [Howard, 2019], and ImageNet [Russakovsky *et al.*, 2015] datasets, using diverse combination of teacher and student pairs. The results show that StableKD consistently outperforms the state of the art by 1% – 18% in absolute accuracy, especially when constrained by a limited amount of training budget. Equipped with StableKD, the Swin-T network [Liu *et al.*, 2021] achieves impressive 82.6% accuracy on ImageNet, much better than its 81.2% counterpart with vanilla KD. When having similar accuracy, StableKD can also speed up the KD process up to 10 \times . For example, StableKD reaches 78.45% accuracy on CIFAR100 with 20 epochs while vanilla KD requires 200 epochs to reach 78.07%. Moreover, our StableKD framework enjoys further benefits of being data-efficient. For example, with only 40% of the CIFAR100 or 60% of the ImageNet training data, StableKD attains comparable or even higher accuracy than vanilla KD with the whole dataset.

To summarize, our contributions are as follows:

- We reveal and verify, for the first time, the IBOE issue commonly occurred in end-to-end KD approaches.
- We present StableKD, a simple yet effective KD framework, to mitigate the IBOE issue.
- We conduct extensive experiments and verify that our StableKD framework is highly accurate, fast, and data-efficient. It is a generic framework and can be applied to various tasks and neural networks.

2 Related Work

Knowledge distillation (KD), introduced by Hinton *et al.* [2015], is a prominent technique for model compression that leverages a large teacher network to guide a smaller student neural network.

network [Hinton *et al.*, 2015; Li *et al.*, 2017, 2021]. Existing works can be broadly classified into two types based on the knowledge transferred: logit-based and feature-based. The former imposes various regularization on the student’s output [Hinton *et al.*, 2015; Zhao *et al.*, 2022; Furlanello *et al.*, 2018; Mirzadeh *et al.*, 2020], while the latter further transfers intermediate representations [Zagoruyko and Komodakis, 2016a; Heo *et al.*, 2019b; Huang and Wang, 2017; Kim *et al.*, 2018; Shen *et al.*, 2019; Guan *et al.*, 2020; Chen *et al.*, 2021a; Romero *et al.*, 2014; Peng *et al.*, 2019; Chen *et al.*, 2021b].

Though promising in transferring diverse knowledge from a teacher to its student, those KD approaches requires intensive computation and time cost to maintain the teacher’s performance [Beyer *et al.*, 2022]. Some recent works have attempted to accelerate the KD process [Yun *et al.*, 2021; Shen and Xing, 2022], for instance, by caching the teacher’s output for later use in the KD process [Shen and Xing, 2022]. However, these approaches incur storage overhead, performance degradation, and limited acceleration rate (usually less than 2 \times). By contrast, our StableKD overcomes these drawbacks and achieves a more substantial improvement in reducing the distillation time.

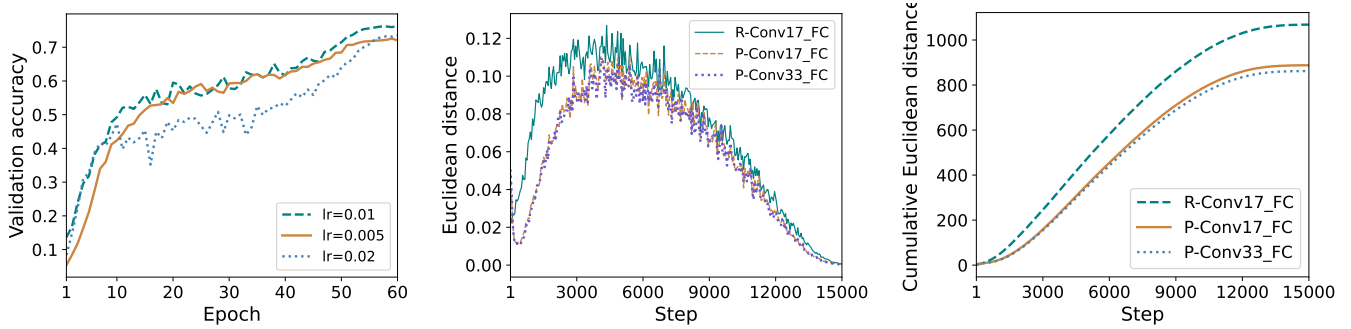
Another line of research is to enhance the data efficiency of KD, by either updating a subset of parameters alternately [Wang *et al.*, 2018; Kulkarni *et al.*, 2019], adding cross data flow as regularization [Bai *et al.*, 2020; Shen *et al.*, 2021], or expanding the training set [Wang *et al.*, 2020; Nguyen *et al.*, 2022; Laskar and Kannala, 2020]. Similar to those works, our StableKD benefits from high data efficiency by enabling blockwise KD. However, our StableKD is much simpler to implement, without complex data or architectural manipulations. Our StableKD is also faster to train, as it performs the blockwise KD almost parallelly.

3 Hypothesis and Experimental Validation

It is commonly believed that the success of deep learning largely lies in the nature of being deep, *i.e.*, the more layers stacked, the better performance a neural network could achieve. However, optimizing very deep neural networks is challenging for various reasons, such as the problems of gradient explosion [Iskoldskii *et al.*, 1977] and gradient vanishing [Hochreiter, 1998]. Specifically, Shalev-Shwartz *et al.* [2017] identify the issue of noisy gradient in end-to-end training, which slows down the convergence significantly. Inspired by this, we investigate the cause of noisy or non-informative gradients and propose the following hypothesis:

The IBOE Hypothesis. *For each block in a randomly-initialized neural network, the randomness of its back-propagated gradients is influenced by the random noises in the parameters of its adjacent blocks. This causes optimization instability, reduces the network accuracy, and delays the convergence, especially when the network is far from mature. We refer to this phenomenon as Inter-block Optimization Entanglement (IBOE).*

To empirically show that IBOE exists, we conduct two simple exploratory experiments: 1) Monitor a student network’s validation accuracy during the vanilla KD process, and check



(a) Validation accuracy increases with fluctuations for most of the epochs and for all runs with different learning rates. (b) The randomly initialized R-Conv17 incurs higher Euclidean distance of the FC parameters, than the pre-trained counterparts. (c) Further supporting the conclusion drawn in (b), yet from the angle of cumulative Euclidean distance.

Figure 2: Results of the preliminary experiments. All point to the soundness of our IBOE hypothesis.

if there’s any fluctuations occurred, as a proxy to qualitatively reflect the optimization stability. 2) Monitor the Euclidean distance between the parameters of two consecutive steps, as another proxy to quantitatively measure the optimization stability [Hardt *et al.*, 2016].

For the first toy experiment, we use the widely-adopted CIFAR100 [Krizhevsky, 2009] dataset, and use the golden ResNet34 and ResNet18 [He *et al.*, 2016] as the teacher and student networks, respectively. We then conduct the vanilla KD (refer to Section 4.1 for more details) for 60 epochs using the SGD optimizer [Paszke *et al.*, 2017] and the OneCycle scheduler [Smith and Topin, 2019]. The base learning rate is set as 0.005, 0.01, and 0.02 for three different runs. From Figure 2(a), we can clearly see that their validation accuracy increases with fluctuations for most of the epochs. One may argue that it is because the step size or the learning rate is too large and overshoots in the optimal direction. However, such fluctuations still exist for relatively smaller learning rate. Indeed, this phenomenon can be interpreted as the consequence of the IBOE issue, where different blocks collaborate but also interfere with each other.

To further validate our hypothesis quantitatively, we conduct the second experiment using three feature extractors: R-Conv17, P-Conv17, and P-Conv33. The prefixes “R-” and “P-” indicate whether a network is randomly initialized or pre-trained, while “Conv17” and “Conv33” denote the convolutional layers of a ResNet18 and a ResNet34, respectively, both excluding the original fully connected (FC) layer. We then attach a new FC layer as the classifier to each of them. Note that the parameters of the three FC layers have the same initial random values. We train them following the similar setting to our first experiment, but now we monitor the Euclidean distance between the FC parameters of two consecutive steps, as well as its cumulative version. As shown in Figure 2 (b) and (c), we highlight three key points:

- 1) With R-Conv17, the classifier FC suffers from larger distances and thereby higher instability than those with P-Conv17 and P-Conv33.
- 2) This gap is much larger in the early training steps.
- 3) P-Conv33 has a similar distance level to P-Conv17,

showing that the optimization stability is less relevant to the network capacity but more restricted by the mature state or noise level of the parameters.

In short, all these results are consistent to our IBOE hypothesis, and motivates our next step to address the issue.

4 StableKD: Stable Knowledge Distillation

This section begins with a brief overview of the vanilla KD method, which is a standard baseline in the field. Next, we present our StableKD framework in detail, focusing on the loss functions and the algorithm design.

4.1 Preliminary: Vanilla KD

The vanilla KD approach proposed by Hinton *et al.* [2015] is well-known for its simplicity and effectiveness. One typical task is the image classification, where a student network learns to imitate a teacher by predicting soft targets, *e.g.*, assigning an image a 0.8 probability of being a cat and a 0.2 probability of being a grassland. We present the mathematical formulation of this process below.

An input image x is fed into a teacher network $f^T(\cdot|\theta^T)$ with parameters θ^T as well as a student network $f^S(\cdot|\theta^S)$ with parameters θ^S . Their outputs are denoted as $\hat{y}^T = \text{Softmax}(f^T(x|\theta^T))$ and $\hat{y}^S = \text{Softmax}(f^S(x|\theta^S))$ correspondingly, which are then compared with the ground truth label y to compute the training loss. Note that the notation of Softmax temperature is ignored for simplicity, where value 1 is used for all experiments in this paper. There are two loss terms involved in the vanilla KD, the cross-entropy (CE) loss and the Kullback–Leibler (KL) divergence. Both serve as a measure of statistical distance, but the former is calculated between \hat{y}^S and y while the latter is between \hat{y}^S and \hat{y}^T , *i.e.*,

$$\ell_{CE} = \mathcal{L}_{CE}(\hat{y}^S, y), \quad (1)$$

$$\ell_{KL} = \mathcal{L}_{KL}(\hat{y}^S, \hat{y}^T). \quad (2)$$

Now the overall vanilla KD loss can be calculated by

$$\mathcal{L}_{KD} = (1 - \alpha)\ell_{CE} + \alpha\ell_{KL}, \quad (3)$$

where $\alpha \in (0, 1)$ is a hyper-parameter balancing the above two loss terms.

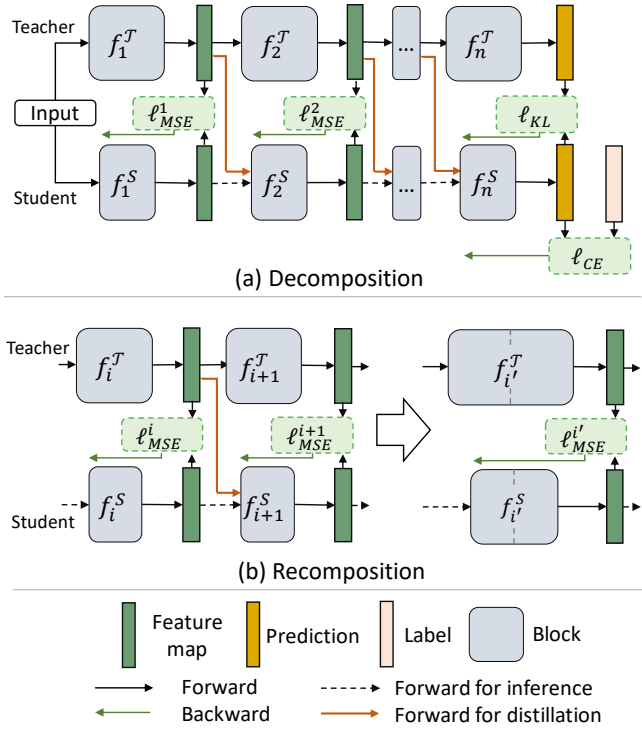


Figure 3: Overview of our StableKD. It has two key operations, *Decomposition* and *Recomposition*. The former divides the teacher and student networks into several pairs of blocks, which then perform the KD process separately for certain epochs. After that, the latter merges the adjacent blocks two by two, followed by a new KD stage.

4.2 Details of StableKD

The above formulation shows that the vanilla KD naively treats the student network as a whole and a black box for end-to-end training, which inherently suffers from the IBOE issue as we have examined in Section 3. Building upon this finding, we introduce StableKD, a simple yet effective KD framework that enables more fine-grained block-wise training to mitigate the IBOE problem. Specifically, our StableKD involves two novel operations *Decomposition* and *Recomposition*. The *Decomposition* operation, as shown in Figure 3 (a), divides a pair of teacher and student networks into several blocks for separate distillation. Note that the intermediate feature maps from the teacher are directed to the subsequent block of the student. By contrast, the *Recomposition* operation, as shown in Figure 3 (b), progressively merges the decomposed blocks back along the training process, to preserve the architectural consistency between training and testing, avoiding potential accuracy drop. To elaborate our workflow more clearly, we next provide a rigorous mathematical description.

Decomposition.

A neural network $f(\cdot|\theta)$ with parameters θ can be decomposed into multiple blocks f_1, f_2, \dots, f_k satisfying $f(\cdot|\theta) = f_k \circ \dots \circ f_2 \circ f_1(\cdot|\theta)$ for some $k \in \mathbb{N}$, where $f \circ g(\cdot) := f(g(\cdot))$.

For simplicity, we denote $\bigcirc_{i=1}^k f_i := f_k \circ f_{k-1} \circ \dots \circ f_1$. As there are different ways of decomposition, we denote \mathcal{D} as

one specific decomposition strategy, which specifies the number of divided blocks k and how these blocks are partitioned from the student and teacher models. \mathcal{D} can be empirically determined and preset at the beginning of StableKD process. In this paper, we consider the FC layer at the end as a single block and divide the remaining layers, e.g., convolutional layers and multi-head attention layers into 2–4 blocks, based on their feature dimensions and receptive fields (refer to appendix for more details).

After the decomposition, we get multiple pairs of teacher and student blocks. Training is then conducted separately for each pair. For the last pair, the training loss is similar to Equation 3, comprising a CE loss and a KL divergence:

$$\ell_{CE} = \mathcal{L}_{CE}(\hat{y}^{T,S}, y), \quad (4)$$

$$\ell_{KL} = \mathcal{L}_{KL}(\hat{y}^{T,S}, \hat{y}^T), \quad (5)$$

where $\hat{y}^{T,S}$ denotes the prediction of the last student block, which relies on its teacher's preceding blocks, i.e., $\hat{y}^{T,S} = \text{Softmax}\left(f_k^S \circ \bigcirc_{i=1}^{k-1} f_i^T(x|\theta^S, \theta^T, \mathcal{D})\right)$. For the remaining pairs of blocks, we adopt the mean squared error (MSE) loss to densely transfer the knowledge. Specifically, the MSE loss ℓ_{MSE}^i for block f_i is written as

$$\ell_{MSE}^1 = \mathcal{L}_{MSE}(f_1^T(x|\theta^T, \mathcal{D}), f_1^S(x|\theta^S, \mathcal{D})), \quad (6)$$

for $i = 1$, and

$$\ell_{MSE}^i = \mathcal{L}_{MSE}\left(\bigcirc_{j=1}^i f_j^T(x|\theta^T, \mathcal{D}), \right. \quad (7)$$

$$\left. f_i^S \circ \bigcirc_{j=1}^{i-1} f_j^T(x|\theta^S, \theta^T, \mathcal{D})\right),$$

for $i = 2, 3, \dots, k-1$. Although different pairs of blocks are trained separately, we can also put all these loss terms together as a summary:

$$\mathcal{L}_{StableKD} = \ell_{CE} + \lambda \ell_{KL} + \sum_{i=1}^{k-1} \ell_{MSE}^i. \quad (8)$$

Overall, Equation (8) enables various kinds of knowledge transfer from the teacher blocks to their corresponding student blocks concurrently yet without interfering with each other. With only a few epochs, the loss shrinks quickly, and the students blocks start to converge.

Recomposition.

While the *Decomposition* operation is designed to alleviate IBOE issue, the divided blocks are blind to each other. This leaves the student an architectural discrepancy between training and testing, and makes the student less accurate during testing, as we verified in Section 5.3. Therefore, we propose to progressively merge the divided blocks back along the training process. To be more concrete, we have the following definition:

Definition 1 (Recomposing Function \mathcal{R}). *Given \mathcal{D} that encodes the information of k blocks decomposed from a teacher or a student network, $\mathcal{R}(\mathcal{D})$ merges the original i -th and $(i+1)$ -th blocks together as a new block for every positive odd number $i \leq k-1$.*

Algorithm 1 StableKD algorithm

Parameter: θ^S, θ^T **Input:** decomposition variable \mathcal{D} , number of recompositions n , number of training epochs for each stage e_i , balancing factor of losses λ

```
1: Initialize  $\theta^S$  and freeze  $\theta^T$ .
2: for training stage  $c = 0, 1, \dots, n$  do
3:   for each of  $e_c$  epochs do
4:     Update  $\theta^S$  with Equation (8).   {Decomposition.}
5:   end for
6:    $\mathcal{D} \leftarrow \mathcal{R}(\mathcal{D})$            {Recomposition.}
7: end for
8: return  $\theta^S$ 
```

In other word, $\mathcal{R}(\cdot)$ is a function taking \mathcal{D} as the input and returning an updated \mathcal{D} , which has $\lceil \frac{k}{2} \rceil$ blocks after recomposition. Figure 3 (b) demonstrates this operation in which $i' = (i + 1)/2$ for $i = 1, 3, \dots, k - 1$, supposing $k - 1$ is an odd number. Every time the recomposing function is performed, our StableKD enters a new stage of training, and finally evolves towards the vanilla KD.

Complete pipeline.

Given the initial decomposition strategy \mathcal{D} and the number of recompositions to perform n , we present the complete pipeline of StableKD in Algorithm 1. The complete pipeline is simple to understand and easy to implement. It’s expected to achieve a higher accuracy and converge faster than vanilla KD. Moreover, our StableKD is as computation-efficient as the vanilla KD for each iteration, by avoiding complex and heavy data and architectural manipulations. Note that we denote **StableKD- k/n** as the full StableKD pipeline with k divided blocks initially and with n recompositions.

5 Experimental Evaluation

In this section, we begin by validating the efficacy of StableKD in mitigating the IBOE issue. We then present empirical evidence showcasing the advantages of StableKD from three practical aspects: convergence speed, accuracy, and data efficiency. Our experimental analyses encompass convolutional neural networks and transformer-based models trained on diverse datasets, such as CIFAR100 [Krizhevsky, 2009], Imagewoof [Howard, 2019], and ImageNet [Russakovsky *et al.*, 2015]. The results illustrate that StableKD achieves superior accuracy compared to previous approaches, while requiring fewer training epochs and reduced training data. Furthermore, we conduct ablation studies to assess the indispensability of the decomposition and recomposition operations in StableKD, and also explore potential avenues for future enhancements.

5.1 StableKD in Alleviating IBOE

This experiment aims to validate the efficacy of StableKD in mitigating the IBOE issue. We adopt the ResNet18 [He *et al.*, 2016] as the student and the ResNet34 with pre-trained accuracy 78.39% as the teacher on CIFAR100. We explore

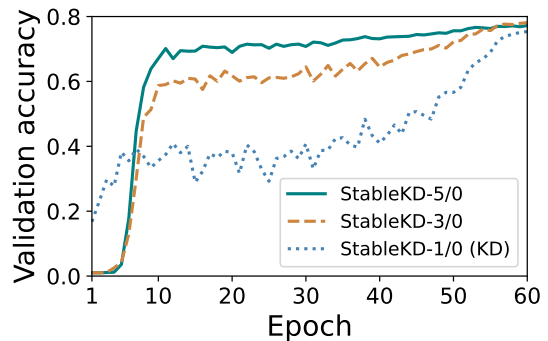


Figure 4: StableKD effectively alleviates the inter-block optimization entanglement.

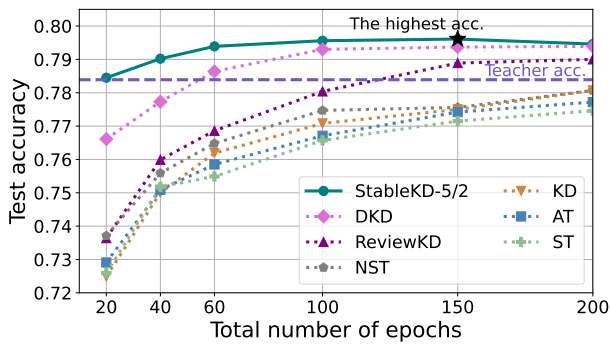
three decomposition strategies with the values of k equal to 1, 3, and 5, while no recompositions are used. Note that setting $k = 1$ is equivalent to the vanilla KD. For all the three runs, we conduct the training for 60 epochs, with a learning rate of 0.05 and a OneCycleLR scheduler [Smith and Topin, 2019]. We monitor their validation accuracies along the training process. Figure 4 shows that the accuracy of vanilla KD or StableKD-1/0 suffer from severe fluctuations, whereas the accuracy of StableKD-5/0 and StableKD-3/0 increase much more stably, effectively circumventing the IBOE issue.

5.2 Illustrative Results

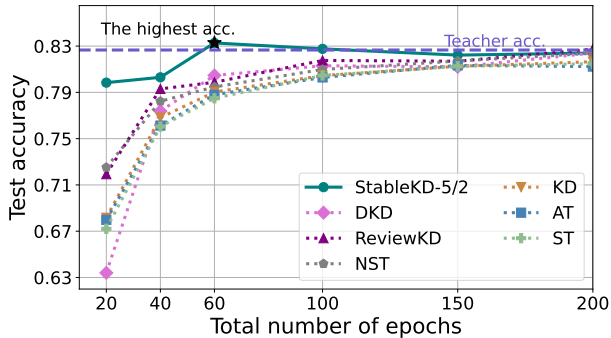
Comparison of convergence speed and accuracy.

In deep learning, the convergence speed generally refers to the number of epochs, iterations, or training time spent in achieving a high level of accuracy. By contrast, the accuracy is often reported given a fixed number of epochs. For comprehensive evaluation, here we mainly compare the trade-offs between the test accuracy and the total number of epochs. We first conduct experiments on CIFAR100 and Imagewoof datasets. We train a ResNet18 with a teacher ResNet34 for 20, 40, 60, 100, 150, and 200 epochs. For StableKD, we set the following hyper-parameters: $k = 5, n = 2, e_0 = \lfloor e/3 \rfloor, e_1 = \lfloor e/3 \rfloor, e_2 = e - 2\lfloor e/3 \rfloor$, where e is the total number of epochs. We compare StableKD against six representative works, including the vanilla KD [Hinton *et al.*, 2015], Attention Transfer (AT; Zagoruyko and Komodakis 2016a), Sobolev Training (ST; Czarnecki *et al.* 2017), Neuron Selectivity Transfer (NST; Huang and Wang 2017), Knowledge Review (ReviewKD; Chen *et al.* 2021b), and Decoupled Knowledge Distillation (DKD; Zhao *et al.* 2022). Results in Figure 5 show that StableKD renews the state of the art, consistently achieving the highest accuracy given varied number of epochs, where the gap is more evident with limited training budget. From another perspective, StableKD converges faster than others in achieving a high accuracy.

These conclusions are consistent when further applied to other teacher-student pairs, *e.g.*, the WRN28-10-WRN16-10 and the ResNeXt38 ($32 \times 4d$)-ResNeXt20 ($32 \times 4d$). Results in Figure 6 show that StableKD speeds up the KD process by $5\times$, from 200 epochs to 40 epochs when trained on CIFAR100. With only 20 epochs, StableKD also obtains a

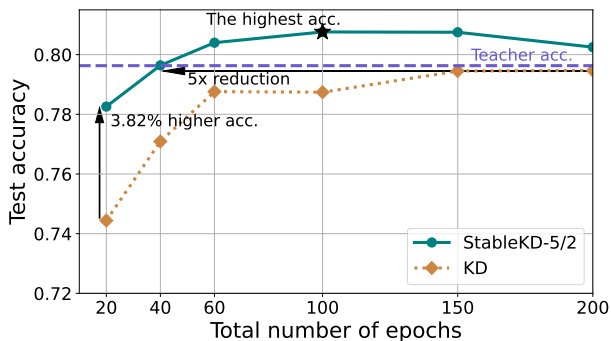


(a) CIFAR100

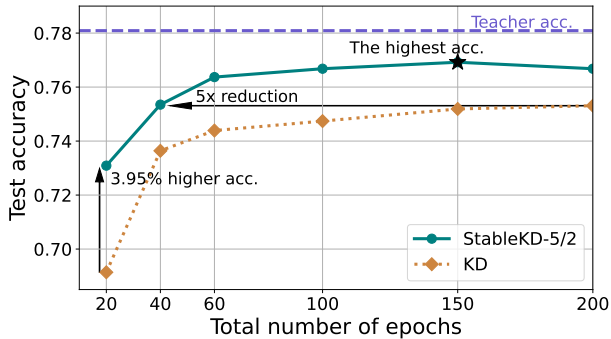


(b) Imagenet

Figure 5: StableKD outperforms others by achieving higher test accuracy with fewer training epochs on CIFAR100 and Imagenet datasets.



(a) WRN16-10 & WRN28-10



(b) ResNeXt20(32 × 4d) & ResNeXt38(32 × 4d)

Figure 6: For different teacher-student pairs, StableKD consistently achieves higher accuracy on CIFAR100 with fewer epochs than the vanilla KD.

Student \mathcal{S}	Teacher \mathcal{T}	Epochs	KD Scheme	Acc. (%)
ViT-S/8	ViT-S/16 (74.03%)	90	w/o KD	74.00
			KD	75.05
			DeiT	75.45
			StableKD-5/3	77.72
Swin-T	Swin-S (83.33%)	90	w/o KD	79.53
			KD	79.95
			StableKD-5/3	81.51
			Swin-T	Swin-S (83.33%)
KD	81.15			
StableKD-5/3	82.61			

Table 1: Performance comparison on the large scale ImageNet dataset. ViT-S/8 denotes a network with depth 8 derived from ViT-S/16. DeiT is designed for ViT and not directly applicable to Swin.

significant 3.8% and 4.0% accuracy gain for the two pairs, respectively.

We also conduct experiments on ImageNet, a much larger scale of classification dataset with 1.2 million images. We use transformer-based backbones including ViT [Dosovitskiy *et al.*, 2020] and Swin [Liu *et al.*, 2021]. Results are summarized in Table 1. Compared to training w/o KD, vanilla KD, and DeiT [Touvron *et al.*, 2021], StableKD improves the accuracy by 2.0% - 3.7% for both 90 and 300 epochs. StableKD-5/3 trained with 90 epochs even beats the vanilla KD method with 300 epochs (81.51% v.s. 81.15%).

Comparison of data efficiency.

We compare the data efficiency by examining how well different KD methods perform with reduced training dataset, from 100% to only 20% of the whole dataset. Other training settings and baselines are the same to previous experiments. We present the results in Table 2. Compared to prior works, StableKD demonstrates significantly higher data efficiency by maintaining robustly good accuracy with varying subset sizes. With 20% of the training data, StableKD outperforms others by a large margin ranging from 6% to 20% in accuracy. Furthermore, StableKD trained with 40% - 60% of the training data performs similarly or even better than others trained with the whole dataset.

It is common practice to pre-train transformer-based models on external data before fine-tuning them on the target dataset to prevent overfitting and improve performance. To further validate the strengths of StableKD in achieving higher data efficiency and thereby reducing the training cost, we trained transformer-based student networks from scratch on CIFAR100 without any pre-training on external data. Results in Table 3 show that all baselines perform poorly while StableKD stands out with 10% - 18% significantly higher accuracy, indicating its superior data efficiency.

5.3 Ablation Studies

Effect of decomposition. To validate the effectiveness of decomposition, we degrade StableKD to conventional feature-based KD methods by imposing the feature alignment but removing the independence of different blocks. We adopt the ResNet18-ResNet34 pair and train the student for 60 epochs. Results in Table 4 show that the feature alignment

Dataset	Student \mathcal{S}	Teacher \mathcal{T}	# epochs	KD Scheme	Acc. (%) for various subset sizes				
					20%	40%	60%	80%	100%
CIFAR100	ResNet18	ResNet34 (78.39%)	300	KD	55.65	67.64	72.88	75.91	78.12
				AT	56.53	67.22	71.99	75.31	77.99
				ST	55.47	67.54	71.87	75.26	77.75
				NST	60.84	69.87	74.36	76.16	78.14
				ReviewKD	62.20	71.25	75.20	77.19	78.97
				DKD	69.76	75.60	77.39	78.77	79.39
			StableKD-5/2	76.10	78.50	79.18	79.63	79.41	
ImageNet	Swin-T	Swin-S (83.33%)	90	w/o KD	66.01	74.98	77.76	78.67	79.53
				KD	69.64	76.10	78.33	79.52	79.95
				StableKD-5/3	76.03	78.87	80.34	80.89	81.51

Table 2: Comparison of data efficiency with varying subsets of the training data.

Student \mathcal{S}	Teacher \mathcal{T}	Scheme	Acc. (%)
ViT-T/8	ViT-T/16 (88.98%)	w/o KD	67.99
		KD	66.46
		DeiT	71.01
		StableKD-5/2	84.18
Swin-T	Swin-S (90.39%)	w/o KD	73.78
		KD	73.84
		StableKD-5/2	83.92

Table 3: Comparison when training transformer-based networks on CIFAR100 from scratch without pre-training on external data. We use 600 training epochs here.

Scheme	KD	KD + MSE	StableKD-5/2
Acc. (%)	76.19	77.15	79.39

Table 4: With feature alignment, KD + MSE is still inferior to StableKD.

through MSE loss does enhance the vanilla KD by 1.0% in accuracy. However, a more substantial improvement of 3.2% is achieved with the implementation of StableKD. This, therefore, substantiates the necessity of our decomposition operation, particularly the importance of enabling *independent* block-wise KD.

Effect of recomposition. We next evaluate the effectiveness of progressively merging the decomposed blocks by training w/ and w/o recomposition. Other training settings remain the same with the previous ablation experiment. Results in Table 5 show that, without recomposition, StableKD-5/0 surpasses the vanilla KD for 20, 40, and 60 epochs due the use of decomposition in accelerating the convergence. However, StableKD-5/0 gets lower accuracy than the vanilla KD for more training epochs. This is because individual blocks are trained independently but lack mutual awareness, leading to sub-optimal accuracy. To address it, we introduce the recomposition procedure, which consistently yields higher accuracy as is evident in the results.

KD schemes	Acc. (%) for various numbers of epochs					
	20	40	60	100	150	200
KD	72.49	75.00	76.19	77.08	77.50	78.07
StableKD-5/0	76.59	76.90	77.26	76.99	77.39	77.23
StableKD-5/2	78.45	79.02	79.39	79.21	79.61	79.46

Table 5: StableKD-5/2 with recomposition consistently obtains higher accuracy than StableKD-5/0 without recomposition and the vanilla KD.

Student	Teacher (Acc., # params)	Projector (# params)	Test accuracy (%)		
			w/o KD	KD	StableKD-2/1
WRN40-2	WRN40-4 (77.11%, 8.9M)	\times (2.2M)	74.56	75.35	n/a
		\checkmark (2.3M)	74.96	75.40	75.61
WRN16-8	WRN16-10 (79.69%, 17.1M)	\times (11.0M)	78.53	78.67	n/a
		\checkmark (11.6M)	78.75	78.73	79.57

Table 6: More results for heterogeneous architectures. The reported accuracies of WRN40-2 and WRN16-8 in their original paper are 73.96% and 77.93%, respectively.

Dealing with heterogeneous feature dimensions. Our main experiments are conducted when the student and teacher networks have the same feature dimension in each block. What if the dimension differs, *e.g.*, having different network width? To address this and extend the application scope of StableKD, we can simply insert additional projectors, *e.g.*, the conv 1×1 layer, within the student network, and thus enable the use of our StableKD. To validate this, we conduct experiments on Wide ResNet [Zagoruyko and Komodakis, 2016b] with varying width factors. We train them on CIFAR100 for 200 epochs. Results in Table 6 demonstrate the promising applicability of StableKD to heterogeneous feature dimensions.

6 Conclusion

In this paper, we have studied and uncovered a common issue of existing KD approaches – the inter-block optimization entanglement that causes their slow convergence and lower accuracy. To overcome it, we have proposed a novel StableKD framework, which divides a pair of teacher and stu-

dent networks into several blocks, and distills the block-wise knowledge separately before combining them together for inference. We have conducted extensive experiments and validated that StableKD is highly accurate, fast-converging, and data-efficient. We hope that our StableKD can make KD more practical as a tool for model compression and acceleration, particularly in the era of building foundation models towards artificial general intelligence.

Appendix

A Limitations and Future Work

We have verified the application of StableKD in image classification across several different neural networks. However, the proposed decomposition can become complex when the model architecture includes longer shortcuts, *i.e.*, operations that pass features from shallow layers to deep ones. For example, networks for semantic segmentation, such as FCN [Long *et al.*, 2015] and U-Net [Ronneberger *et al.*, 2015], often concatenate features from shallow and deep layers to enhance performance. Since our proposed StableKD primarily focuses on dividing blocks in a sequential order, the exploration of non-sequential neural networks remains an open area for future work.

B Training Details

Learning rate scheduler. We propose a novel scheduler to enable per-training-stage warm-up and annealing. Intuitively, our learning rate extends the concepts from the cyclical learning rate [Smith, 2017] in PyTorch CyclicalLR with *triangular2* strategy; that is, instead of using cycles with same number of epochs, each cycle corresponds to the number of epochs in each StableKD stage. Illustration can be found in Figure 7. For other comparison schemes, we use a OneCycle scheduler [Smith and Topin, 2019] in the CIFAR100 and Imgewoof experiments (Figure 5, 6, Table 2, 3, 4, 5, 6), and a cosine-annealing scheduler with linear warm-up in the ImageNet experiments (Table 1,2). Note that all experiments in Figure 4 are conducted with a OneCycle scheduler.

Optimizer. We adopt SGD as the optimizer in the CIFAR100 and Imgewoof experiments (Figure 4, 5, 6, Table 2, 3, 4, 5, 6), and use AdamW for the ImageNet experiments (Table 1, 2).

Hyperparameters. Our empirical experience recommends a higher learning rate for StableKD. In the CIFAR100 and Imgewoof experiments, all the experiments are conducted with a batch size of 128 and weight decay of $5e - 4$. The maximal learning rate of StableKD is set to 0.5. For other comparison schemes, we use a maximal learning rate of 0.1, where they demonstrate better performance and thus serve as stronger baselines. In the ImageNet experiments, we set the maximal learning rate, batch size, and weight decay to $2e - 2$, 256, $2e - 1$ for StableKD, and to $2e - 3$, 512, $4e - 2$ for other schemes, respectively. We found that StableKD generally performs better when a larger learning rate, a smaller batch size, and a smaller weight decay are used. This differs

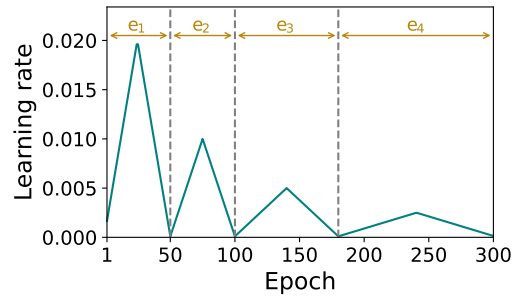


Figure 7: Learning rate scheduler used in StableKD.

from previous works, which a smaller batch size usually accompanies a larger weight decay and a smaller learning rate. We attribute this difference to the benefits of higher stability that make the model easier to train.

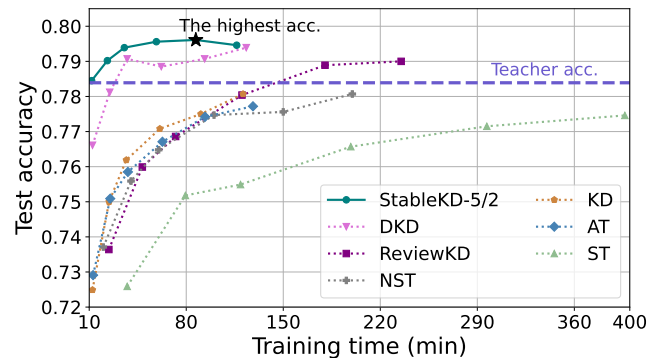


Figure 8: Comparison of accuracy on CIFAR100 with the ResNet34-ResNet18 pair.

KD schemes	Average time per epoch (s)	
	CIFAR100	Imgewoof
KD	36.3	14.9
AT	37.5	15.6
ST	120.6	44.7
NST	60.0	30.0
ReviewKD	72.0	28.4
DKD	37.3	15.3
StableKD-5/2	35.4	14.7

Table 7: Comparison of time cost per epoch with the ResNet34-ResNet18 pair.

C Time Cost

StableKD has low computational complexity and is easy to implement, as no overlapping backward process takes place in the student network. Table 7 shows the average training time per epoch on the CIFAR100 and Imgewoof datasets, with a teacher ResNet34 and a student ResNet18 on a single RTX-2080Ti GPU. With these results, we can also adjust the horizontal axis of Figure 5 to display time cost for clearer

visualization. For example, Figure 8 shows the results on CIFAR100 with the same teacher-student pair.

D Decomposition Details

This paragraph describes the decomposition recipes of StableKD in the main paper. In our experiment, we regard the last MLP layer as a single block. For ResNet [He *et al.*, 2016], Wide ResNet [Zagoruyko and Komodakis, 2016b], and ResNeXt [Xie *et al.*, 2017] models, we divide the convolutional layers based on the dimension of each residual block. For example, the first decomposed block of ResNet18 in StableKD-5/n consists of the layers from first convolution layer to the last one with an output channel of 64. The second, third, and fourth blocks include the layers with output channels of 128, 256, and 512, respectively. The fifth block represents the fully-connected layer. A similar recipe is used in ResNet34 as well. For Swin models, we follow the division method in its original paper [Liu *et al.*, 2021], where the attention layers are decomposed into blocks with depths of 2, 2, 6, 2 in Swin-T, and 2, 2, 18, 2 in Swin-S. For ViT models [Dosovitskiy *et al.*, 2020], the attention layers are equally distributed to the first four blocks of StableKD-5/n, and the last block contains the fully-connected layer.

References

- Haoli Bai, Jiaxiang Wu, Irwin King, and Michael Lyu. Few shot network compression via cross distillation. In *Proceedings of the AAAI Conference on Artificial Intelligence*, volume 34(04), pages 3203–3210, 2020.
- Lucas Beyer, Xiaohua Zhai, Amélie Royer, Larisa Markeeva, Rohan Anil, and Alexander Kolesnikov. Knowledge distillation: A good teacher is patient and consistent. In *Proceedings of the IEEE/CVF Conference on Computer Vision and Pattern Recognition*, pages 10925–10934, 2022.
- Defang Chen, Jian-Ping Mei, Yuan Zhang, Can Wang, Zhe Wang, Yan Feng, and Chun Chen. Cross-layer distillation with semantic calibration. In *Proceedings of the AAAI Conference on Artificial Intelligence*, volume 35(8), pages 7028–7036, 2021.
- Pengguang Chen, Shu Liu, Hengshuang Zhao, and Jiaya Jia. Distilling knowledge via knowledge review. In *Proceedings of the IEEE/CVF Conference on Computer Vision and Pattern Recognition*, pages 5008–5017, 2021.
- Wojciech M Czarnecki, Simon Osindero, Max Jaderberg, Grzegorz Swirszcz, and Razvan Pascanu. Sobolev training for neural networks. *Advances in Neural Information Processing Systems*, 30, 2017.
- Jacob Devlin, Ming-Wei Chang, Kenton Lee, and Kristina Toutanova. Bert: Pre-training of deep bidirectional transformers for language understanding. *arXiv preprint arXiv:1810.04805*, 2018.
- Alexey Dosovitskiy, Lucas Beyer, Alexander Kolesnikov, Dirk Weissenborn, Xiaohua Zhai, Thomas Unterthiner, Mostafa Dehghani, Matthias Minderer, Georg Heigold, Sylvain Gelly, et al. An image is worth 16x16 words: Transformers for image recognition at scale. *arXiv preprint arXiv:2010.11929*, 2020.
- Tommaso Furlanello, Zachary Lipton, Michael Tschannen, Laurent Itti, and Anima Anandkumar. Born again neural networks. In *International Conference on Machine Learning*, pages 1607–1616. PMLR, 2018.
- Yushuo Guan, Pengyu Zhao, Bingxuan Wang, Yuanxing Zhang, Cong Yao, Kaigui Bian, and Jian Tang. Differentiable feature aggregation search for knowledge distillation. In *Computer Vision—ECCV 2020: 16th European Conference, Glasgow, UK, August 23–28, 2020, Proceedings, Part XVII 16*, pages 469–484. Springer, 2020.
- Moritz Hardt, Ben Recht, and Yoram Singer. Train faster, generalize better: Stability of stochastic gradient descent. In *International conference on machine learning*, pages 1225–1234. PMLR, 2016.
- Kaiming He, Xiangyu Zhang, Shaoqing Ren, and Jian Sun. Deep residual learning for image recognition. In *Proceedings of the IEEE conference on computer vision and pattern recognition*, pages 770–778, 2016.
- Byeongho Heo, Jeesoo Kim, Sangdoon Yun, Hyojin Park, Nojun Kwak, and Jin Young Choi. A comprehensive overhaul of feature distillation. In *Proceedings of the IEEE/CVF International Conference on Computer Vision*, pages 1921–1930, 2019.
- Byeongho Heo, Minsik Lee, Sangdoon Yun, and Jin Young Choi. Knowledge transfer via distillation of activation boundaries formed by hidden neurons. In *Proceedings of the AAAI Conference on Artificial Intelligence*, volume 33(01), pages 3779–3787, 2019.
- Geoffrey Hinton, Oriol Vinyals, Jeff Dean, et al. Distilling the knowledge in a neural network. *arXiv preprint arXiv:1503.02531*, 2(7), 2015.
- Sepp Hochreiter. The vanishing gradient problem during learning recurrent neural nets and problem solutions. *International Journal of Uncertainty, Fuzziness and Knowledge-Based Systems*, 6(02):107–116, 1998.
- Sean D Holcomb, William K Porter, Shaun V Ault, Guifen Mao, and Jin Wang. Overview on deepmind and its alphago zero ai. In *Proceedings of the 2018 international conference on big data and education*, pages 67–71, 2018.
- Jeremy Howard. Imagenette/imagenet, 2019.
- Zehao Huang and Naiyan Wang. Like what you like: Knowledge distill via neuron selectivity transfer. *arXiv preprint arXiv:1707.01219*, 2017.
- AM Iskol'skii, Iu E Nesterikhin, Aleksandr Zaharovich Patashinskii, Vladimir Kirillovich Pinus, and Ia G Epelbaum. On the instability of a gradient explosion. In *Akademiia Nauk SSSR Doklady*, volume 236, pages 1346–1349, 1977.
- Sangwon Jung, Donggyu Lee, Taeon Park, and Taesup Moon. Fair feature distillation for visual recognition. In *Proceedings of the IEEE/CVF conference on computer vision and pattern recognition*, pages 12115–12124, 2021.

- Jangho Kim, SeongUk Park, and Nojun Kwak. Paraphrasing complex network: Network compression via factor transfer. *Advances in neural information processing systems*, 31, 2018.
- Alex Krizhevsky. Learning multiple layers of features from tiny images. *Tech Report*, 2009.
- Akshay Kulkarni, Navid Panchi, Sharath Chandra Raparthy, and Shital Chidharwar. Data efficient stagewise knowledge distillation. *arXiv preprint arXiv:1911.06786*, 2019.
- Zakaria Laskar and Juho Kannala. Data-efficient ranking distillation for image retrieval. In *Proceedings of the Asian Conference on Computer Vision*, 2020.
- Quanquan Li, Shengying Jin, and Junjie Yan. Mimicking very efficient network for object detection. In *Proceedings of the IEEE conference on computer vision and pattern recognition*, pages 6356–6364, 2017.
- Zheng Li, Jingwen Ye, Mingli Song, Ying Huang, and Zhigeng Pan. Online knowledge distillation for efficient pose estimation. In *Proceedings of the IEEE/CVF international conference on computer vision*, pages 11740–11750, 2021.
- Ze Liu, Yutong Lin, Yue Cao, Han Hu, Yixuan Wei, Zheng Zhang, Stephen Lin, and Baining Guo. Swin transformer: Hierarchical vision transformer using shifted windows. In *Proceedings of the IEEE/CVF international conference on computer vision*, pages 10012–10022, 2021.
- Jonathan Long, Evan Shelhamer, and Trevor Darrell. Fully convolutional networks for semantic segmentation. In *Proceedings of the IEEE conference on computer vision and pattern recognition*, pages 3431–3440, 2015.
- Seyed Iman Mirzadeh, Mehrdad Farajtabar, Ang Li, Nir Levine, Akihiro Matsukawa, and Hassan Ghasemzadeh. Improved knowledge distillation via teacher assistant. In *Proceedings of the AAAI conference on artificial intelligence*, volume 34(04), pages 5191–5198, 2020.
- Dang Nguyen, Sunil Gupta, Kien Do, and Svetha Venkatesh. Black-box few-shot knowledge distillation. In *European Conference on Computer Vision*, pages 196–211. Springer, 2022.
- Adam Paszke, Sam Gross, Soumith Chintala, Gregory Chanan, Edward Yang, Zachary DeVito, Zeming Lin, Alban Desmaison, Luca Antiga, and Adam Lerer. Automatic differentiation in pytorch. In *NIPS-W*, 2017.
- Baoyun Peng, Xiao Jin, Jiaheng Liu, Dongsheng Li, Yichao Wu, Yu Liu, Shunfeng Zhou, and Zhaoning Zhang. Correlation congruence for knowledge distillation. In *Proceedings of the IEEE/CVF International Conference on Computer Vision*, pages 5007–5016, 2019.
- Adriana Romero, Nicolas Ballas, Samira Ebrahimi Kahou, Antoine Chassang, Carlo Gatta, and Yoshua Bengio. Fitnets: Hints for thin deep nets. *arXiv preprint arXiv:1412.6550*, 2014.
- Olaf Ronneberger, Philipp Fischer, and Thomas Brox. U-net: Convolutional networks for biomedical image segmentation. In *International Conference on Medical image computing and computer-assisted intervention*, pages 234–241. Springer, 2015.
- Olga Russakovsky, Jia Deng, Hao Su, Jonathan Krause, Sanjeev Satheesh, Sean Ma, Zhiheng Huang, Andrej Karpathy, Aditya Khosla, Michael Bernstein, et al. Imagenet large scale visual recognition challenge. *International journal of computer vision*, 115:211–252, 2015.
- Shai Shalev-Shwartz, Ohad Shamir, and Shaked Shammah. Failures of gradient-based deep learning. In *International Conference on Machine Learning*, pages 3067–3075. PMLR, 2017.
- Zhiqiang Shen and Eric Xing. A fast knowledge distillation framework for visual recognition. In *European Conference on Computer Vision*, pages 673–690. Springer, 2022.
- Chengchao Shen, Xinchao Wang, Jie Song, Li Sun, and Mingli Song. Amalgamating knowledge towards comprehensive classification. In *Proceedings of the AAAI Conference on Artificial Intelligence*, volume 33(01), pages 3068–3075, 2019.
- Chengchao Shen, Xinchao Wang, Youtan Yin, Jie Song, Sihui Luo, and Mingli Song. Progressive network grafting for few-shot knowledge distillation. In *Proceedings of the AAAI Conference on Artificial Intelligence*, volume 35 (3), pages 2541–2549, 2021.
- Leslie N Smith and Nicholay Topin. Super-convergence: Very fast training of neural networks using large learning rates. In *Artificial intelligence and machine learning for multi-domain operations applications*, volume 11006, pages 369–386. SPIE, 2019.
- Leslie N Smith. Cyclical learning rates for training neural networks. In *2017 IEEE winter conference on applications of computer vision (WACV)*, pages 464–472. IEEE, 2017.
- Hugo Touvron, Matthieu Cord, Matthijs Douze, Francisco Massa, Alexandre Sablayrolles, and Hervé Jégou. Training data-efficient image transformers & distillation through attention. In *International conference on machine learning*, pages 10347–10357. PMLR, 2021.
- Hui Wang, Hanbin Zhao, Xi Li, and Xu Tan. Progressive blockwise knowledge distillation for neural network acceleration. In *IJCAI*, pages 2769–2775, 2018.
- Dongdong Wang, Yandong Li, Liqiang Wang, and Boqing Gong. Neural networks are more productive teachers than human raters: Active mixup for data-efficient knowledge distillation from a blackbox model. In *Proceedings of the IEEE/CVF Conference on Computer Vision and Pattern Recognition*, pages 1498–1507, 2020.
- Saining Xie, Ross Girshick, Piotr Dollár, Zhuowen Tu, and Kaiming He. Aggregated residual transformations for deep neural networks. In *Proceedings of the IEEE conference on computer vision and pattern recognition*, pages 1492–1500, 2017.
- Sangdoon Yun, Seong Joon Oh, Byeongho Heo, Dongyoon Han, Junsuk Choe, and Sanghyuk Chun. Re-labeling imagenet: from single to multi-labels, from global to localized labels. In *Proceedings of the IEEE/CVF Conference*

- on *Computer Vision and Pattern Recognition*, pages 2340–2350, 2021.
- Sergey Zagoruyko and Nikos Komodakis. Paying more attention to attention: Improving the performance of convolutional neural networks via attention transfer. *arXiv preprint arXiv:1612.03928*, 2016.
- Sergey Zagoruyko and Nikos Komodakis. Wide residual networks. *arXiv preprint arXiv:1605.07146*, 2016.
- Borui Zhao, Quan Cui, Renjie Song, Yiyu Qiu, and Jiajun Liang. Decoupled knowledge distillation. In *Proceedings of the IEEE/CVF Conference on computer vision and pattern recognition*, pages 11953–11962, 2022.